

# Rheological behavior of coextruded multilayer architectures

D. R. BEEAFF, G. E. HILMAS

Department of Ceramics Engineering, University of Missouri-Rolla, Rolla, MO 65409, USA  
E-mail: dbeeaff@umr.edu

Utilizing a thermoplastic extrusion process, a multilayered architecture was fabricated. Thermoplastic blends of 55 vol% X7R dielectric and 50 vol% nickel powder were prepared by high shear mixing. Sheets pressed from this material were cut, stacked, and laminated to produce multilayered blocks. The blocks were extruded through a slotted spinneret to reduce layer thickness. The relation between viscosity and shear rate is relatively well understood for two- or three-layered polymer coextrusion. This behavior has not been studied for heavily loaded multi-component systems, such as might be used for MLCCs and other multilayered devices. A correlation was observed between the flow behavior during extrusion and that observed during mixing. Results show how control of the rheological behavior of highly loaded systems can control extrusion defects.

© 2002 Kluwer Academic Publishers

## 1. Introduction

The drive towards smaller dielectric layers in capacitors is driven by the volumetric energy density equation:

$$E_d(J \cdot m^{-3}) = 1/2 \varepsilon_0 K [V/t]^2 \quad (1)$$

where,  $\varepsilon_0 = 8.85 \times 10^{-12} F \cdot m^{-1}$ ,  $K$  = dielectric constant,  $V$  = applied potential,  $t$  = dielectric thickness.

The equation states that the volumetric energy density,  $E_d$ , is proportional to  $1/t^2$ . That is, as the dielectric layer becomes thinner, the ability to hold an electric charge increases. However, an additional consequence of this reduced layer thickness is that the electric field across the layer increases as well, leading to increased chance of dielectric breakdown. Therefore, high energy density storage devices rely on thick dielectric layers. Current methods for the manufacturing of multilayer ceramic capacitors (MLCCs) typically involve tape casting technologies [1–7]. To fabricate thick dielectric devices via tape casting requires the lamination of multiple layers until a sufficient thickness is reached. As the requirement for dielectric layer thickness in multilayer capacitors becomes more stringent, the ability to fabricate devices with micron sized layers becomes correspondingly more difficult using traditional tape casting techniques.

To address these issues, researchers at UMR have developed a coextrusion process for the fabrication of multilayer architectures with offset electrodes. The process utilizes high shear blending of ceramic powders, as the dielectric layers, and metal powders as the electrode, with a thermoplastic polymer. Sheets of the materials are cut to size and alternately stacked in the desired geometry. These stacks are then coextruded until the desired dielectric layer thickness is achieved. The pro-

gram has focused on base metal electrode MLCCs, utilizing doped barium titanate for the dielectric material along with nickel for the electrode.

The first step in achieving these results is to blend the ceramic powder with a thermoplastic binder using a high shear mixer. Rheological properties can be influenced by powder characteristics such as particle size, shape and surface chemistry as well as effects of dispersants, mixing rate and temperature [8–11]. Sheets of the resulting material are cut and stacked to form a multilayer feedrod, which is then extruded to reduce layer thickness.

Multilayer flow through a die is sensitive to extrusion rate. In addition to typical extrusion flaws such as melt fracture and stick-slip, multilayer flows may exhibit instability at the layer interfaces [12]. This results from the tendency of the lowest viscosity material to migrate towards the region of highest shear, i.e. the die wall [13]. In simpler, two layer extrudates this can result in an “encapsulation” defect in which one material surrounds the other [14]. Since the relation between shear rate and viscosity is material dependent, the material that migrates toward the die wall can vary with extrusion rate. The object of the present study was to investigate this phenomenon for extrudates containing a large quantity of multilayers.

## 2. Experimental procedure

### 2.1. Starting materials

The doped  $BaTiO_3$  (APS  $1 \mu m$ ) powder was TAMTRON X7R292N (Ferro Corp., Niagara Falls, NY). The nickel powder (APS  $1 \mu m$ ) was Cerac N-2003 (Cerac, Inc., Milwaukee, WI). The binders used were poly(ethylene-*co*-butyl acrylate) (Aldrich Chemical Company, Milwaukee, WI), poly(ethylene ethyl acrylate) (Union Carbide Corp., Danbury, CT), and

TABLE I Binder formulations for dielectric and electrode layers

Material	Density ( $\text{g} \cdot \text{cm}^{-3}$ )	Vol%
Barium titanate	5.50	52.5
PEBA (7 wt% butyl acrylate)	0.92	32.5
Microcrystalline wax	0.80	11.0
Heavy mineral oil	0.89	4.0
Nickel	8.90	50
PEBA (35 wt% butyl acrylate)	0.93	32.5
Poly(ethylene ethyl acrylate)	0.90	7.5
Microcrystalline wax	0.80	10.0
PEG-dioleate	0.89	<1

microcrystalline wax (ExxonMobile, Irving, TX). Thermoplastics have been typically used for injection molding applications and the process of blending the binders and powders is well established for common structural ceramics such as alumina [15–19].

## 2.2. Mixing

A Brabender high-shear mixer (C.W. Brabender, Hackensack, NJ) was used to blend the powders and thermoplastic binders according to the formulations given in Table I. The mixer was heated above the thermoplastic softening point, typically  $130^{\circ}\text{C}$ . Binders were added and allowed to blend for 10 minutes. The powder was added slowly, along with a plasticizing agent. The volume of the mixture was formulated to be 42 cc (70% of the total mixer volume), with the composition being about 50 vol% solids. After all ingredients had been added the material was removed and mixed again for one half hour at 25 RPM and a temperature of  $150^{\circ}\text{C}$  to improve homogeneity and reduce particle agglomeration.

## 2.3. Lamination

The mixture from the Brabender was placed between two Mylar® sheets, which in turn were placed between two steel caul plates, and set on a 50-ton hydraulic press with heated platens (Wabash, Model No. G50H-18-CX). Using steel shims to maintain thickness, the material was pressed to 0.254 mm thickness sheets. The material can be pressed to thinner sheets, but for the purpose of these experiments, the thickness remained 0.254 mm. The X7R sheets were cut into  $25.4 \text{ mm} \times 63.5 \text{ mm}$  and  $6.35 \text{ mm} \times 63.5 \text{ mm}$  strips and the nickel sheets were cut into  $19.05 \text{ mm} \times 63.5 \text{ mm}$  strips. The strips were then stacked by hand as shown in Fig. 1. Each offset nickel layer is separated by two dielectric layers. This process was repeated until a  $25.4 \text{ mm} \times 25.4 \times 63.5 \text{ mm}$  square rod was fabricated. These layers were then heated in a die to  $140^{\circ}\text{C}$  and pressed at 700 lbs force to laminate the layers and produce a solid feedrod.

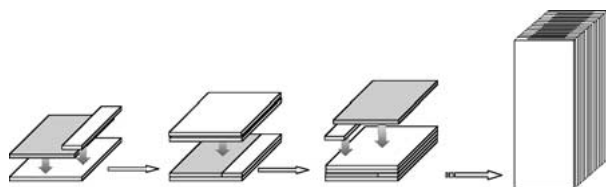


Figure 1 Schematic of multi-layered feedrod assembly.

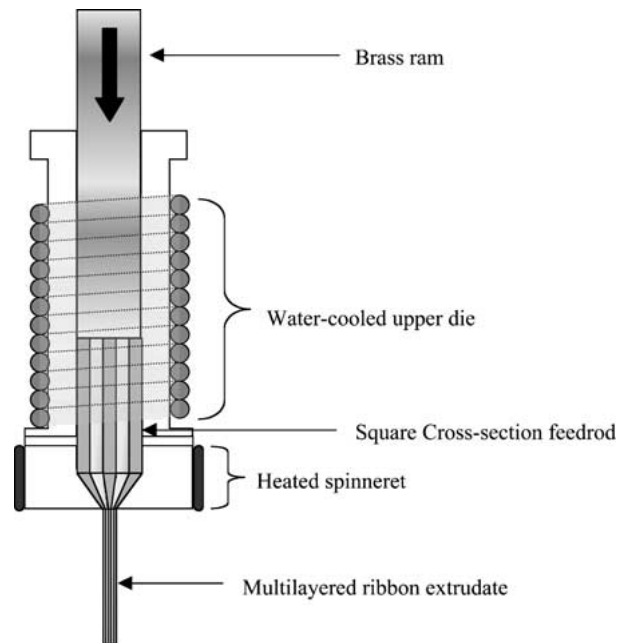


Figure 2 Schematic of extrusion die used to coextrude multilayer feedrod.

This step is currently the most time consuming of the entire process as it relies on hand lay-up. Other researchers have developed coextrusion processes utilizing manifold dies and other schemes to allow for semi-continuous coextrusion, bypassing much of the manual labor [20–23]. While this approach is fully applicable to the process presented here, the tooling costs associated with a manifold capable of offset electrodes was outside the scope of the program.

## 2.4. Coextrusion

Fig. 2 shows a schematic of the die used to extrude the  $\text{BaTiO}_3/\text{Ni}$  system. The multilayer block produced during the lamination process was placed into an extrusion die and heated. A 5-ton piston extruder was used to extrude the laminated feedrod through a  $24.4 \text{ mm} \times 2.54 \text{ mm}$  rectangular spinneret. Extrusion was performed at  $120^{\circ}\text{C}$  with a ram speed of 0.1 to 4 mm/min. A load cell mounted between the motor drive shaft and the brass piston recorded the force required for extrusion. From this data, a linear plot could again be obtained of extrusion rate (shear rate) vs. extrusion load (shear force). The extrudate was cut to  $25.4 \text{ mm}$  squares, with a thickness approximately 2.54 mm. Die swell caused a 8% linear increase in thickness relative to the die orifice size.

## 3. Results and discussion

### 3.1. Mixing

Each batch was mixed twice to improve homogeneity and mixed for 30-minute during the second batching. Agglomerates are known to increase the torque during mixing, primarily by increasing the relative volume fraction of solids [24]. However, the high shear experienced during mixing can cause the breakdown of agglomerates [25, 26], which is reflected as a decrease and stabilization in torque readings. It should be noted that a decrease can also be attributed to thermal scission of the polymer binder at higher temperatures [27],

so temperature stability is important during the mixing step. Most polymeric flow behavior can be modeled using a non-linear (e.g., non-Newtonian) power law relation between shear stress,  $\tau$ , and shear rate,  $\dot{\gamma}$ , given by the equation:

$$\tau = K \dot{\gamma}^n \quad (2)$$

where  $K$  and  $n$  are rheological constants. It can be shown that there is a relation between the shear stress, the torque moment,  $M_t$ , of the mixer blades and the volume of mixture. Combining this relation with the above equation yields:

$$M_t = \frac{3}{2} V K \dot{\gamma}^n \quad (3)$$

Furthermore, the shear rate can be calculated from the velocity of the mixer blade edge,  $u$ , and the space,  $h$ , between the blade edge and the mixer wall. This is given by the equation:

$$\dot{\gamma} = \frac{u}{h} = \frac{d\pi R}{60h} \quad (4)$$

in which  $R$  is the mixer rate in revolutions per minute and  $d$  is the blade diameter. Substituting this equation, taking the log of both sides and rearranging gives:

$$\log M = \log\left(\frac{3}{2} V K\right) + n \log\left(\frac{\pi d}{60h} R\right) \quad (5)$$

If we define a new rheological mixing constant,  $C_m$ , such that:

$$C_m = \log\left(\frac{3}{2} V K\right) + n \log\left(\frac{\pi d}{60h}\right) \quad (6)$$

Then the equation further simplifies to:

$$\log M = n \log R + C_m \quad (7)$$

This equation is practical because it allows one to plot the logarithm of torque versus the logarithm of mixing speed, providing a linear relationship with a slope of equal to the power law exponent,  $n$ . It is possible also to calculate the apparent viscosity, since  $\eta_a = \tau/\dot{\gamma}$ . For a power law fluid, this mean apparent viscosity can be found from  $\eta_a = K \dot{\gamma}^{(n-1)}$ . However, the approach taken simplifies the complex shape of the mixing blades by replacing them with a cylindrical approximation. In reality, there is a distribution of viscosities within the mixing chamber [28]. Calculation of apparent viscosity also requires an estimation of the parameter  $K$ , which in this case is an empirical constant. The Hershel-Bulkley model ( $\tau = \tau_y + K \dot{\gamma}^n$ ) [29] is simply a power law model which incorporates a yield stress and some researchers have derived semi-empirical expressions to replace the empirical  $K$  parameter [30, 31], which have proven useful for fluids which exhibit Newtonian flow at low shear rates. It is also important to note that a simple power law relationship fails at high solids loadings

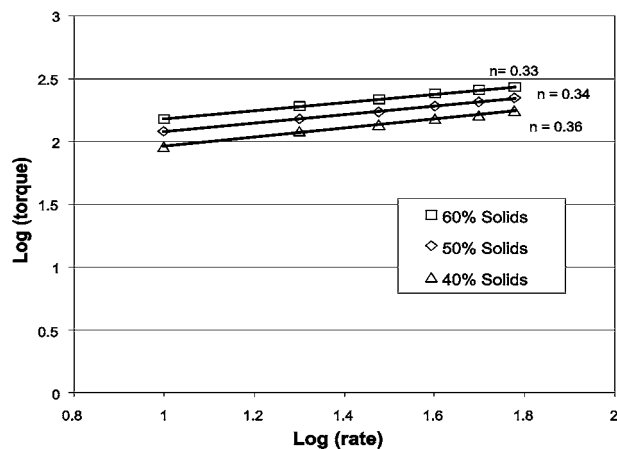


Figure 3 Torque-shear rate plot for X7R powder at various solids loadings at 150°C.

(>62 vol%) in many systems due to particle-particle interactions and other models must be applied [32]. However, for our purposes, in which the solids loading is ~50 vol%, such an empirical Hershel-Bulkley model is suitable.

Fig. 3 shows the log(torque) vs. log(rate) graph for the PEBA-7/Wax binder at various loading of X7R powder. Power law exponents can be determined by fitting a line to the data points and calculating the slope. The graph demonstrates that the barium titanate/thermoplastic material is shear thinning. Nickel-loaded batches were determined to be shear thinning as well, with  $n$  approximately 0.1, a point which will become important in the discussion that follows.

### 3.2. Coextrusion

The technique is based on coextrusion of a multi-component material system consisting of thermoplastic binders and ceramic powders [33, 34]. The ability to coextrude bi- or multi-material systems is inherently dependent on the relative viscosity of each component [12–14, 35, 36]. Any variation will result in rearrangement of the interface and instability during extrusion [14]. In this program, the most common defect that results from such a mismatch is the “hourglass” effect, in which the barium titanate material migrates toward the corners of the extrusion die drawing electrode material with it. This flow initiates a migration of material from the edges of extrudate towards the center. This results in an hourglass appearance of the offset electrode configuration in cross-section, as shown in Fig. 4.

To explore the origin of these defects, batches of both materials were produced and separately extruded through the slotted extrusion die. In this arrangement, the piston extruder functions in a similar fashion to a capillary rheometer. The flow mechanics of capillary rheometry have been studied in depth and it is the method typically used to characterize fluid flow [37–42]. The same power law relationship exists between the shear rate and the shear force, in this case the ram load. The nickel material required a greater load to extrude material at an equal rate to the barium titanate material. Fig. 5 shows a plot of the logarithm of load versus the logarithm of extrusion rate.

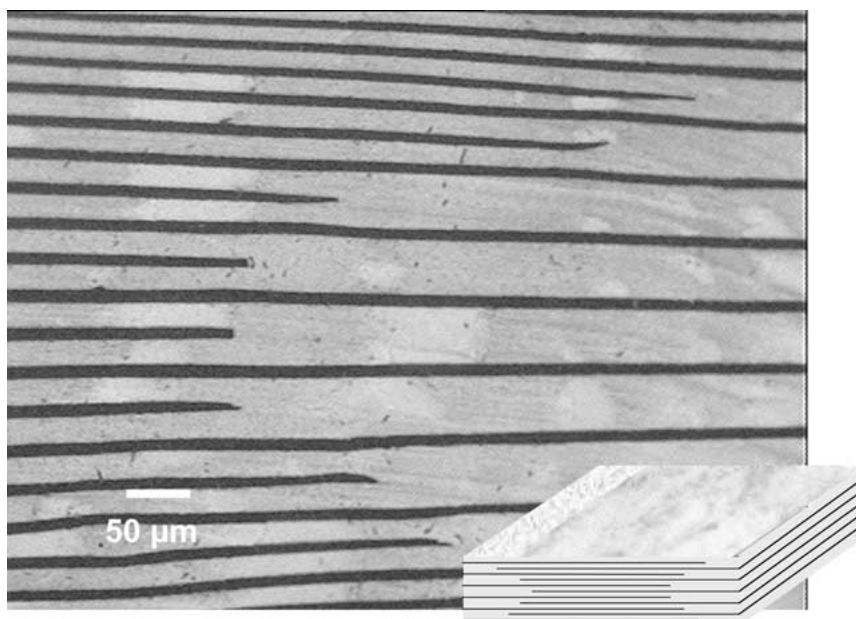


Figure 4 Cross-section of extruded ribbon showing progressively displaced electrodes. Vertical symmetry gives the appearance of an hourglass shape as indicated by inset schematic.

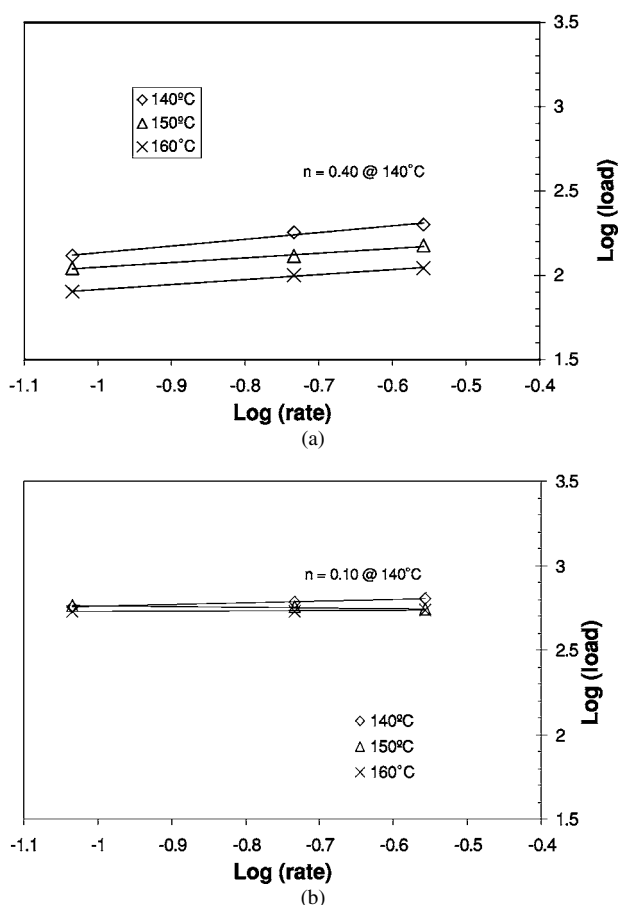


Figure 5 Load-extrusion rate plot for (a) X7R and (b) nickel powders at various temperatures.

The nickel material is exceptionally shear thinning (the power law exponent,  $n$ , is  $\sim 0.1$ ) whereas the dielectric material is only moderately shear thinning ( $n = 0.3$ ). This becomes an issue since the shear rate during extrusion is  $\sim 0.05 \text{ sec}^{-1}$  while the shear rate during mixing is on the order of  $\sim 50 \text{ sec}^{-1}$ . Based on this flow behavior, the difference of three orders of magnitude between shear rates observed between the

mixer and the extruder could be expected to produce the deleterious effects observed during coextrusion.

The cause of the “hourglass” defect is thus found to be due to the comparatively low viscosity of the barium titanate material at the reduced shear rate observed during extrusion. As shown in Fig. 5, the shear-thinning behavior of the dielectric and electrode binders is dissimilar. At a low extrusion rate (typically  $< 1 \text{ mm} \cdot \text{sec}^{-1}$  ram speed), the shear rate at the die wall is not sufficient to cause the barium titanate to migrate. However at slightly higher rates ( $> 2 \text{ mm} \cdot \text{sec}^{-1}$  ram speed), the hourglass shape begins to form, increasing in severity with even higher extrusion rates. At the proper extrusion rate ( $< 1.5 \text{ mm} \cdot \text{sec}^{-1}$  ram speed), spreading of the near-surface layers is not observed nor is there any significant dielectric binder migration towards the die corners.

From this, we can explain the origin of the coextrusion defects. The lowest viscosity material will flow to the region of highest shear rate. In this case, during extrusion the barium titanate material is the lowest viscosity material and flows towards the corners. This causes material along the edges to compress and flow towards the center. The result is the “hourglass” effect and low viscosity material accumulation in the corners. This is shown schematically in Fig. 6.

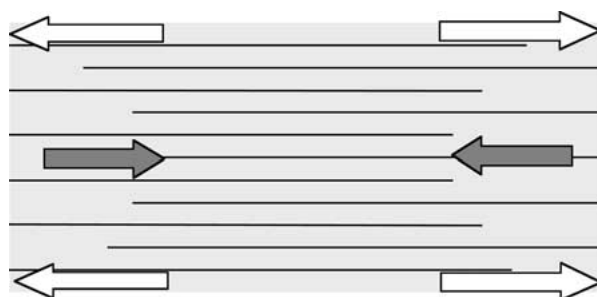


Figure 6 Schematic of cross sectional mass flow during extrusion, which results in layer displacement shown in Fig. 4.

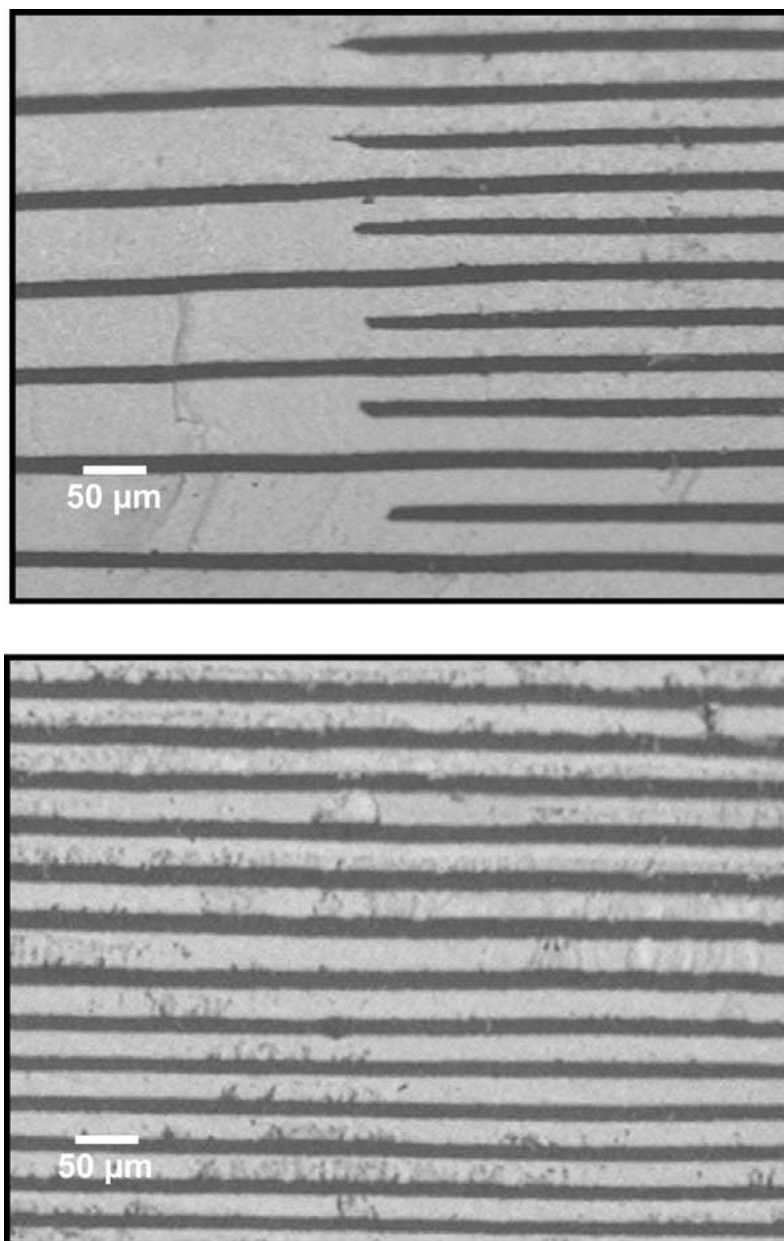


Figure 7 Cross section of successfully coextruded ribbon showing non-displaced electrode layers.

An extrusion rate of  $<1 \text{ mm} \cdot \text{sec}^{-1}$  crosshead speed results in a low enough shear rate that spreading of the barium titanate material does not occur. As shown in Fig. 7, the offset electrode edges are not displaced while the dielectric layer thickness remains constant.

#### 4. Summary

Coextrusion of highly loaded, multi-component systems is a novel approach to forming multilayered structures. The rheological behavior of the composite system during extrusion is fundamental importance. An understanding of the rheology of each system constituent was vital in eliminating or controlling detrimental defects introduced during the coextrusion process. Controlling the relative viscosities of the constituents is important in complex multilayer structures. Large dielectric layer thickness was used for these rheological experiments. The method is limited primarily to the particle size of the starting powders, as the technique has been used to produce green dielectric and electrode layer thickness

as thin as  $10 \mu\text{m}$ , simply by using thinner sheets during the lamination stage [43].

The process is time consuming only for the fact that a portion relies on intensive hand pressing, cutting, and lay-up. This could be avoided through the use of continuous extrusion processes. Additionally, the final process step of cutting the extrudate leaves the electrode edges exposed (no pullback), which will lead to component failure under high fields. Concurrent research suggests that this can be alleviated by coating the part with a high dielectric strength polymer or glass [43].

#### References

1. G. MAHER, in "Ceramic Thin and Thick Films," Vol. 11, edited by B. V. Hiremath (American Ceramic Society, Westerville, OH, 1990) p. 429.
2. J. WILSON, J. ARTHUR and T. JAENECKE, *Ceramic Industry* **9** (1993) 51.
3. L. E. CROSS, in "Handbook of Solid State Batteries and Capacitors," edited by M. Z. A. Munshi (World Scientific, Singapore, 1995) p. 663.
4. J. M. WILSON, *Am. Cer. Soc. Bull.* **74**(6) (1996) 106.

5. S. L. SWARTZ, T. R. SHROUT and T. TAKENAKA, *ibid.* **76**(7) (1997) 59.
6. *Idem.*, *ibid.* **76**(7) (1997) 51.
7. S.-F. WANG, *J. Amer. Ceram. Soc.* **82**(10) (1999) 2677.
8. B. C. MUTSUDDY, *Proc. Brit. Cer. Soc.* **33** (1983) 117.
9. J. H. SONG and J. R. G. EVANS, *J. Rheology* **40**(1) (1996) 131.
10. R. W. FORD, R. A. SCOTT and R. J. B. WILSON, "Effect of Processing on Flow Properties of some Linear Polyethylene Resins" *J. Appl. Polym. Sci.* **12** (1968) 547.
11. S. J. MONTE and G. SUGERMAN, *Poly. Eng. & Sci.* **24**(18) (1984) 1369.
12. W. MICHAELI, "Extrusion Dies for Plastics" (Hanser Publishers, Munich, 1992).
13. N. MINAGAWA and J. L. WHITE, *Poly. Eng. and Sci.* **15**(12) (1975) 825.
14. T. I. BUTLER, *Tappi Journal* (1992) 205.
15. M. TAKAHASHI, S. SUZUKI, H. NITANADA and E. ARAI, *J. Amer. Ceram. Soc.* **71**(12) (1988) 1093.
16. S. T. LIN and R. M. GERMAN, *J. Mater. Sci.* **29** (1994) 5207.
17. T. CHAN and S. LIN, *J. Amer. Ceram. Soc.* **78**(10) (1995) 2746.
18. J. H. SONG and J. R. G. EVANS, *Ceramics Int'l.* **21** (1995) 325.
19. R. RAMAN, W. SLIKE III and R. M. GERMAN, *Cer. Eng. Sci. Proc.* **14**(11/12) (1993) 166.
20. T. SHANNON and S. BLACKBURN, *ibid.* **16** (1995) 1115.
21. Z. LIANG and S. BLACKBURN, *ibid.* **20**(4) (1999) 47.
22. *Idem.*, *ibid.* **20**(4) (1999) 587.
23. C. D. MUELLER, S. NAZARENKO, T. EBELING, T. L. SHUMAN, A. HILTNER and E. BAER, *Poly. Eng. and Sci.* **37**(2) (1997) 355.
24. J. H. SONG and J. R. G. EVANS, *J. Mater. Sci. Lett.* **13** (1994) 1642.
25. H. BÖHM and S. BLACKBURN, *J. Mat. Sci.* **29** (1994) 5779.
26. R. D. WILDMAN and S. BLACKBURN, *ibid.* **33** (1998) 5119.
27. R. W. FORD, R. A. SCOTT and R. J. B. WILSON, *J. Appl. Polym. Sci.* **11** (1967) 547.
28. L. L. BLYLER and J. H. DAANE, *Poly. Eng. And Sci.* (1967) 178.
29. W. H. HERSHEL and R. BULKLEY, *Kolloid, Z.* **39** (1926) 249.
30. H. TANAKA and J. L. WHITE, *J. Non-Newt. Fl. Mech.* **7** (1980) 333.
31. A. J. POSLINKSI, M. E. RYAN, R. K. GUPTA, S. G. SESHADRI and F. J. FRECHETTE, *J. Rheology* **32**(7) (1988) 703.
32. N. Q. DZUY and D. V. BOGER, *ibid.* **27**(4) (1983) 321.
33. C. VAN HOY, A. BARDA, M. GRIFFITH and J. W. HALLORAN, *J. Amer. Ceram. Soc.* **81**(1) (1998) 152.
34. A. BRADY, G. HILMAS and J. W. HALLORAN, in "Ceramic Transactions," Vol. 51, edited by H. Hausner and G. Messing (American Ceramic Society, Westerville, OH, 1995) p. 321.
35. W. A. GIFFORD, *Poly. Eng. Sci.* **37**(2) (1997) 315.
36. S. LEVY and J. F. CARLEY, (eds.), "Plastics Extrusion Technology Handbook" (Industrial Press, New York, 1989) p. 223.
37. TADMOR, ZEHER, GUGOS and G. COSTAS, "Principles of Polymer Processing" (John Wiley & Sons, New York, 1979) p. 524.
38. J. J. BENBOW, T. A. LAWSON, E. W. OXLEY and J. BRIDGWATER, *Cer. Bull.* **68**(10) (1989) 1821.
39. J. ZHENG, W. B. CARLSON and J. S. REED, *J. Amer. Ceram. Soc.* **75**(11) (1992) 3011.
40. R. J. HUZZARD and S. BLACKBURN, *Powder Tech.* (1998) 118.
41. S. BLACKBURN, H. MILLS and N. EL-BAKHBAKHI, *Brit. Cer. Trans.* **97**(5) (1998) 205.
42. J. J. BENBOW, S. BLACKBURN and H. MILLS, *J. Mater. Sci.* **33** (1998) 5827.
43. D. BEEAFF and G. HILMAS, unpublished work.

*Received 1 August 2000  
and accepted 15 May 2001*